RAMP1 in Kupffer cells is a critical regulator in immune-mediated hepatitis

Tomoyoshi Inoue[1,2,3¶], Yoshiya Ito[1,3¶], Nobuyuki Nishizawa[1,4], Koji Eshima[5], Ken Kojo[5], Fumisato Otaka[1,2,3], Tomohiro Betto[1,2,3], Sakiko Yamane[1,2,3], Kazutake Tsujikawa[6], Wasaburo Koizumi[2], and Masataka Majima[1,3*]

¶ These authors contributed equally to this work.

[1]Department of Molecular Pharmacology, Graduate School of Medical Sciences, Kitasato University, Sagamihara, Kanagawa 252-0374, Japan,
Departments of [2]Gastroenterology, [3]Pharmacology, [4]Surgery, and [5]Immunology, Kitasato University School of Medicine, Sagamihara, Kanagawa 252-0374, Japan, and
[6]Laboratory of Molecular and Cellular Physiology, Graduate School of Pharmaceutical Sciences, Osaka University, Osaka, Japan

*Correspondence to: Masataka Majima, MD, PhD, Department of Pharmacology, Kitasato University School of Medicine, 1-15-1 Kitasato, Minami-ku, Sagamihara, Kanagawa 252-0374, Japan.
E-mail: mmajima@med.kitasto-u.ac.jp; Phone: +81-42-778-8822; Fax: +81-42-778-9114

Short title; RAMP1 in immune-mediated hepatitis

Abstract

The significance of the relationship between the nervous and immune systems with respect to disease course is increasingly apparent. Immune cells in the liver and spleen are responsible for the development of acute liver injury, yet the regulatory mechanisms of the interactions remain elusive. Calcitonin gene-related peptide (CGRP), which is released from the sensory nervous system, regulates innate immune activation via receptor activity-modifying protein 1 (RAMP1), a subunit of the CGRP receptor. Here, we show that RAMP1 in Kupffer cells (KCs) plays a critical role in the etiology of immune-mediated hepatitis. RAMP1-deficient mice with concanavalin A (ConA)-mediated hepatitis, characterized by severe liver injury accompanied by infiltration of immune cells and increased secretion of pro-inflammatory cytokines by KCs and splenic T cells, showed poor survival. Removing KCs ameliorated liver damage, while depleting T cells or splenectomy led to partial amelioration. Adoptive transfer of splenic T cells from RAMP1-deficient mice led to a modest increase in liver injury. Co-culture of KCs with splenic T cells led to increased cytokine expression by both cells in a RAMP1-dependent manner. Thus, immune-mediated hepatitis develops via crosstalk between immune cells. RAMP1 in KCs is a key regulator of immune responses.

Introduction

The liver is exposed to high concentrations of products derived from the diet and gut microbiota, which in combination with bacterial endotoxins would normally trigger immune responses. Hepatic resident macrophages, called Kupffer cells (KCs), are the principal macrophages in the liver, where they reside in the sinusoids and are thus in a perfect position to monitor materials emanating from the intestine [1]. The liver is innervated by sympathetic, parasympathetic, and peptidergic nerves that contain both afferent and efferent nerve fibers. A number of neuropeptides are present in liver [2]. For example, neuronal fibers expressing substance P and calcitonin gene-related peptide (CGRP) are abundant in the tunica media of vessels in portal tracts, as well as in intra-lobular connective tissue [3]. The nervous system plays a major role in regulating immune homeostasis and inflammation, and the significance of the crosstalk between the nervous and immune systems with respect to injury outcome and/or disease course is increasingly apparent [4].

The immune system is tightly regulated by the nervous system, which releases several mediators (including neurotransmitters). CGRP, a 37 amino acid peptide, is produced in the neural body of dorsal root ganglion cells and released from sensory nerve endings [5]. CGRP binds to a specific receptor, a complex formed by receptor

activity-modifying protein 1 (RAMP1) and calcitonin receptor-like receptor (CRLR) [6]. Binding of CGRP to its receptor triggers an increase in intracellular cyclic adenosine monophosphate levels, leading to vasodilation and transmission of pain signals [5,7]. Because CGRP receptors are expressed by immune cells, CGRP modulates immune responses via receptor binding [5]. Recent studies show that CGRP regulates the function of T cells [8], dendritic cells [9], and macrophages [10] during inflammation. CGRP suppresses production of tumor necrosis factor (TNF)α by lipopolysaccharide (LPS)-activated dendritic cells, thereby increasing production of interleukin (IL)-10 [9]. CGRP exerts similar immunosuppressive actions on T cells and macrophages in the colon [10]. These findings indicate that RAMP1 signaling and immune cells engage in crosstalk, thereby regulating immune responses.

In the liver, CGRP-deficient (*Calca*$^{-/-}$) mice with immune-mediated hepatitis exhibit aggravated liver injury caused by concanavalin A (ConA), which enhances apoptosis mediated by interferon gamma (IFNγ) [11]. ConA hepatitis is mediated by activation of immune cells, including T lymphocytes [12] and KCs [13,14]. Because CGRP and its receptors are expressed in the liver [15] as well as spleen [16,17], RAMP1 signaling regulates ConA hepatitis via immune cells in the liver and spleen. However, it remains unknown about the contribution of RAMP1 signaling in the liver and spleen to the

progression of immune-mediated hepatitis.

Here, we used RAMP1 knockout (*Ramp1*$^{-/-}$) mice to explore the crosstalk between RAMP1 signaling and innate immunity in the liver and spleen during ConA-mediated hepatitis [9,18]. The results indicate that the initial liver injury is driven by interactions between splenic T cells and KCs, and that RAMP1 signaling in KCs orchestrates development of immune-mediated hepatitis. Thus, RAMP1 in KCs is a key modulator during development of immune-mediated hepatitis.

Materials and methods

Animals

Male C57Bl/6 WT mice were obtained from Clea Japan (Tokyo, Japan). Male *Ramp1*$^{-/-}$ mice were developed previously [9]. Mice were maintained at constant humidity (60 ± 5%) and temperature (25 ± 1°C) on a 12 h light/dark cycle. All animals were provided with food and water *ad libitum*. All experimental procedures were approved by the Animal Experimentation and Ethics Committee of the Kitasato University School of Medicine (2017-59), and were performed in accordance with the guidelines for animal experiments set down by the Kitasato University School of Medicine, which are in

accordance with the "Guidelines for Proper Conduct of Animal Experiments" published by the Science Council of Japan. Mice used for survival studies were examined by animal care takers and the overall health status was checked by trained professionals. Mice were euthanized by pentobarbital sodium when they were found in a moribund state as identified by inability to maintain upright position and/or labored breathing. The mice for in vivo experiments were constantly watched throughout the experiment periods. Tissue collection procedures were performed under anesthesia with pentobarbital sodium. At the end of the experiments, the animals were euthanized by exsanguination under anesthesia with pentobarbital sodium followed by cervical dislocation.

Animal procedures

Animals were fasted overnight and then intravenously (i.v.) injected (via the tail vein) with 20 mg/kg Con A (Merck KGaA, Darmstadt, Germany) dissolved in warm pyrogen-free saline (final concentration, 2.0 mg/ml) to induce hepatitis [18]. Mice were anaesthetized with pentobarbital sodium (60 mg/kg, intraperitoneally (i.p.)) at 0, 1, 3, 6, and 24 h after ConA administration (n = 6 for each time point), and blood was drawn. Levels of ALT were measured using a Dri-Chem 7000 Chemistry Analyzer System

(Fujifilm, Tokyo, Japan). Immediately after blood collection, livers were excised and rinsed in saline. A small section of each liver was placed in 10% formaldehyde; the remaining liver was frozen in liquid nitrogen and stored at -80°C. For survival experiment, WT or *Ramp1*$^{-/-}$ mice were treated with ConA (n = 20 per group) and were monitored every 12 h up until 48 h after ConA administration. Some animals received a single subcutaneous injection of CGRP (5.0 µg/mouse in 200 µl of saline; Peptide Institute, Inc. Osaka, Japan) 30 min before treatment with Con A [15] or vehicle (saline).

Neutralization of TNFα and IFNγ

In another set of experiments, mice were injected i.p. with 100 µg of a neutralizing monoclonal antibody specific for mouse TNFα (eBioscience, San Diego, CA, USA) and 100 µg of a neutralizing monoclonal antibody specific for mouse IFNγ (eBioscience) 30 min before ConA administration.

Depletion of CD4+ T cells

Experimental animals were depleted of CD4+ cells using a rat anti-mouse CD4 monoclonal IgG2b antibody (clone GK1.5; BioLegend, San Diego, CA, USA). The

antibody was administered i.p. (300 μg per mouse) 24 h before ConA administration. Control animals were treated with IgG isotype control antibodies (BioLegend).

Depletion of macrophages

Mice were injected i.v. with clodronate CL (200 μl/mouse; FormuMax Scientific, Inc., CA, USA) before 48 h ConA injection. Control groups were injected with control anionic liposomes (200 μl).

Histology and immunohistochemistry

Excised liver tissues were fixed immediately with 10% formaldehyde prepared in 0.1 M sodium phosphate buffer (pH 7.4). Sections (3.5 μm thick) were prepared from paraffin-embedded tissues and either stained with hematoxylin and eosin (H&E) or immunostained with appropriate antibodies. Images of H&E-stained sections were captured under a microscope (Biozero BZ-7000 Series; KEYENCE, Osaka, Japan). Necrosis (expressed as a percentage of the total area) was estimated by measuring the necrotic area in the entire histological section using ImageJ software (US National Institutes of Health, Bethesda, MD, USA).

Immunofluorescence analysis

Tissue samples were fixed with periodate-lysine-paraformaldehyde fixative at room temperature for 3 h. Following cryoprotection with 30% sucrose prepared in 0.1 M phosphate buffer (pH 7.2), sections (8 μm thick) were cut in a cryostat and incubated with Dako Protein Block Serum-Free solution (Glostrup, Denmark) at room temperature for 1 h to block non-specific binding. Sections were then incubated overnight at 4°C with a rabbit anti-mouse RAMP1 polyclonal antibody (Bioss Antibodies, Inc., Woburn, MA, USA), a rat anti-mouse Ly6C monoclonal antibody (Bio-Rad Laboratories, Inc., Puchheim, Germany), a rat anti-mouse CD4 monoclonal antibody (Bio-Rad Laboratories, Inc.), a rat anti-mouse CD3 monoclonal antibody (Bio-Rad Laboratories, Inc.), or a rat anti-mouse CD68 monoclonal antibody (Bio-Rad Laboratories, Inc.). After washing three times in PBS, the sections were incubated with a mixture of the following secondary antibodies for 1 h at room temperature: Alexa Fluor® 488-conjugated donkey anti-rat IgG, Alexa Fluor® 594-conjugated donkey anti-rabbit IgG, Alexa Fluor® 488-conjugated donkey anti-goat IgG (all from Molecular Probes, OR, USA), and Alexa Fluor® 594-conjugated goat anti-guinea pig IgG (Abcam plc, MA, USA). These antibodies were diluted in Antibody Diluent with Background-Reducing Components (Agilent, CA, USA). As a negative control, sections

were incubated in Antibody Diluent with Background-Reducing Components in the absence of a primary antibody. Images were captured under a fluorescence microscope (Biozero BZ-9000 Series; KEYENCE). After labeling, six low-power optical fields (200× magnification) were randomly selected and the number of positive cells was counted. At least five animals were analyzed per marker.

Real-time RT-PCR

Transcripts encoding *Ramp1*, *Calcrl*, *Calca*, *Tnf*, *Ifng*, *Ccl2*, *Ccl5*, *Ccl7*, and glyceraldehyde-3-phosphate dehydrogenase (*Gapdh*) were quantified by real-time RT-PCR analysis. Total RNA was extracted from mouse tissues and homogenized in TRIzol reagent (Life Technologies, Carlsbad, CA, USA). Single-stranded cDNA was generated from 1 μg of total RNA via reverse transcription using the ReverTra Ace® qPCR RT Kit (TOYOBO Co., Ltd., Osaka, Japan), according to the manufacturer's instructions. Quantitative PCR amplification was performed using SYBR Premix Ex Taq™ II (Tli RNaseH Plus; Takara Bio, Inc. Shiga, Japan). The gene-specific primers used for real-time RT-PCR were designed using Primer 3 software (http://primer3.sourceforge.net/) based on data from GenBank. The primers were as follows: 5'-CCATCTCTTCATGGTCACTGC-3' (sense) and

5'-AGCGTCTTCCCAATAGTCTCC-3' (antisense) for *Ramp1*; 5'-CTTCTGGATGCTCTGTGAAGG-3' (sense) and 5'-CCCAGCCGAGAAAATAATACC-3' (antisense) for *Calcrl*; 5'-TCTTCTCATTCCTGCTTGTGG-3' (sense) and 5'-GATCTGAGTGTGAGGGTCTGG-3' (antisense) for *Tnf*; 5'-ATCTGGAGGAACTGGCAAAAG-3' (sense) and 5'-CGCTTATGTTGTTGCTGATGG-3' (antisense) for *Ifng*; 5'-CGGAACCAAATGAGATCAGAA-3' (sense) and 5'-TTGTGGAAAAGGTAGTGGATG-3' (antisense) for *Ccl2*; 5'-CTGCTGCTTTGCCTACCTCTC-3' (sense) and 5'-GTGACAAACACGACTGCAAGA-3' (antisense) for *Ccl5*; 5'-TGCTTTCAGCATCCAAGTGTG-3' (sense) and 5'-ACCGACTACTGGTGATCCTTC-3' (antisense) for *Ccl7*; 5'-ACATCAAGAAGGTGGTGAAGC-3' (sense) and 5'-AAGGTGGAAGAGTGGGAGTTG-3' (antisense) for GAPDH. Data were normalized to GAPDH expression levels.

Measurement of CGRP by ELISA

The concentrations of CGRP in liver and spleen tissues were measured with an ELISA kit (USCN Life Science Inc., Huston, TX, USA), according to the manufacturer's instructions.

Isolation of leukocytes from liver and spleen

Mice were anesthetized with pentobarbital sodium solution (60 mg/kg, i.p.), and the liver was perfused with perfusion buffer (10 ml, 1× Hank's balanced salt solution) through the portal vein. Excised livers were placed immediately at room temperature in RPMI, minced into small pieces using scissors, and incubated in RPMI containing 0.05% collagenase (Type IV; Sigma Chemical Co., St. Louis, MO, USA) at 37°C for 20 min. The tissue was then pressed through a 70 μm cell strainer. The cells were centrifuged at 2600 rpm for 10 min at 4°C, and pelleted cells were resuspended in PBS. Hepatic leukocytes were isolated from liver homogenates by density-gradient centrifugation on 33% Percoll™ (GE Healthcare Life Sciences, Piscataway, NJ, USA), as previously reported [19,20]. Non-parenchymal cells were collected from the interface between the 33% and 66% Percoll™ density cushions and centrifuged at 2700 rpm for 30 min at 4°C. The spleen was also collected and placed immediately in ice-cold RPMI. The tissue was pressed through a 70 μm cell strainer, and erythrocytes were disrupted in

lysis buffer. Viable, nucleated cells were counted by trypan blue exclusion and diluted to a uniform cell density.

Cell culture and co-culture conditions

F4/80+ cells were isolated from the liver and spleen using the mouse F4/80+ Isolation Kit (Miltenyi Biotec, Auburn, CA, USA), according to the manufacturer's instructions. Then, F4/80+ cells were cultured in RPMI 1640 medium containing 10% fetal calf serum and plated in 6-well plates (1.0×10^6 cells per well). After 24 h, cells were stimulated for 3 h with ConA (2 μg/ml) with or without CGRP (1 or 10 nM) (Peptide Institute) in RPMI 1640 medium. CD4+ cells were isolated from the spleen using the mouse CD4+ T cell Isolation Kit (Miltenyi Biotec), according to the manufacturer's instructions. Isolated CD4+ cells (10^6 cells/ml) were stimulated with 1 mg/ml anti-CD3 (BioLegend) and 1 mg/ml anti-CD28 (BioLegend). After 24 h, cells were stimulated for 1 h with ConA with or without CGRP (Peptide Institute) in RPMI 1640 medium. For the co-culture experiments, isolated KCs from liver and/or isolated CD4+ T cells from spleen were seeded into plates. The co-culture was maintained for 24 h, after which co-cultured cells were incubated for 1 h with or without ConA (2 μg/ml) in the presence/absence of CGRP (1 or 10 nM) in advanced RPMI 1640 (Thermo Fisher

Scientific, Inc. Waltham, MA, USA). The F4/80+ cells and CD4+ cells were then harvested and homogenized in TRIzol (Life Technologies), and mRNA levels were measured by real-time RT-PCR.

Flow cytometry analysis

Cells were incubated with the 2.4G2 mAb (anti-cγRIII/II) to block non-specific binding of the primary mAb. Then, cells were stained with a combination of the following fluorochrome-conjugated antibodies: anti-CD45 (clone 30-F11, BioLegend), anti-Ly6G (clone 1A8, BioLegend), anti-Ly6C (clone HK 1.4, BioLegend), anti-CD11b (clone M1/70, BioLegend), anti-F4/80 (clone A3-1, Bio-Rad), anti-CD3 (clone 17A2, BioLegend), anti-CD4 (clone GK1.5, BioLegend), and anti-CD8 (clone 53-6.7, BioLegend). Tubes were placed in the dark on ice for 30 min. Pellets were washed twice with PBS. For flow cytometric analysis, cells were initially gated on forward-scatter (FSC) and side-scatter (SSC) and then gated on CD45+ cells. Cells positive for 7-aminoactinomycin D (7-AAD; BioLegend) were electronically gated from the analysis as dead cells. Samples were measured on a FACSVerse™ (BD, Franklin Lakes, NJ, USA). The data were analyzed using Kaluza software v1.3 (Beckman Coulter, Brea, CA, USA) [19,20]. For intracellular cytokine staining, cells

were incubated for 4 h at room temperature with Golgi Plug (BD Biosciences, San Jose, CA, USA) to block intracellular protein transport. Then, cells were incubated with the 2.4G2 mAb. Saturating concentrations of APC-labeled anti-F4/80 (clone A3-1, Bio-Rad) and APC/Cy7-labeled anti-CD4 (clone GK1.5, BioLegend) antibodies were added. Following washing, cells were fixed and permeabilized prior to intracellular staining of cytokines. After fixation and permeabilization, cells were incubated with PE-labeled anti-TNFα (BioLegend) and FITC-labeled anti-IFNγ (BioLegend) antibodies.

Adoptive transfer of T cells

Isolated splenic CD4-positive cells (T cells) from WT and *Ramp1*$^{-/-}$ mice were injected into WT mice (i.v. at a dose of 5×10^6 cells/200 µl of PBS). Seven days later, recipient mice were treated with ConA. At 24 h post-treatment, serum and liver samples were collected for analyses.

Splenectomy

For splenectomy, the abdominal wall of mice was opened through a left subcostal minimal incision under ether anesthesia. The splenic arteries and veins were ligated at

290 the splenic hilum using 3–0 silk and then divided. The resected spleen was removed,
291 and the abdominal incision was closed. All surgical procedures were performed under
292 sterilized conditions. For the sham operation, the abdominal wall was similarly opened
293 and then closed immediately after identifying the spleen.

294

295 Statistical analysis

296 All results are expressed as the mean ± standard deviation (SD). All statistical analyses
297 were performed using GraphPad Prism software, version 6.07 (GraphPad Software, La
298 Jolla, CA, USA). Unpaired two-tailed Student's t-test was used to compare data
299 between two groups, and one-way analysis of variance, followed by Bonferroni's
300 post-hoc test, was used to compare data between multiple groups. The survival rates of
301 WT and *Ramp1*$^{-/-}$ mice were compared using Kaplan-Meier survival analysis and
302 log-rank tests. A P-value < 0.05 was considered statistically significant.

303

304 Results

305

306 ConA-mediated hepatitis is exacerbated in *Ramp1*$^{-/-}$ mice

307 To elucidate the functional role of RAMP1 signaling during immune-mediated liver

injury, we treated WT and *Ramp1*$^{-/-}$ mice with ConA. First, we examined the impact of RAMP1 deficiency on ConA-induced mortality by monitoring survival every 12 h up until 48 h after ConA administration. We found that 40% of *Ramp1*$^{-/-}$ mice died within 24 h, whereas all of the WT mice survived (Fig 1A). These results suggest that *Ramp1*$^{-/-}$ mice are highly susceptible to acute liver injury caused by ConA. Based on these results, we compared WT and *Ramp1*$^{-/-}$ mice within 24 h of ConA treatment in all subsequent experiments.

Next, we examined the role of RAMP1 signaling in ConA-induced hepatitis by biochemical and histological evaluation of liver injury. Within 6 h of ConA treatment, ALT levels in WT mice began to increase and were elevated markedly at 24 h post-treatment (Fig 1B). By contrast, liver injury in *Ramp1*$^{-/-}$ mice was more severe than that in WT mice, as reflected by markedly higher ALT levels. The same was true for hepatic necrosis, as indicated by the larger necrotic areas in the liver of *Ramp1*$^{-/-}$ mice (Fig 1B and S1 Fig).

Because inflammatory cells, including T cells and macrophages, are responsible for development of ConA hepatitis via production of pro-inflammatory cytokines, we examined accumulation of inflammatory cells in the liver and spleen. Immunofluorescence analysis revealed that, at 24 h after ConA treatment, accumulation

of inflammatory cells (including Ly6C+, CD68+, and CD4+ cells) in *Ramp1*$^{-/-}$-livers was much higher than that in WT livers (Fig 1C and S1 Fig). During the early phase of ConA hepatitis, the number of hepatic CD3+ cells increased minimally (S1 Fig). Next, we examined the recruited inflammatory cells using flow cytometry analysis (Fig 1D 1E, S2 Fig). Exposure to ConA for 24 h caused hepatic accumulation of monocytes (defined as Ly6C^{high}/CD11b^{high}/F4/80^{low}) or recruited macrophages (Ly6C^{high}/CD11b^{high}/F4/80^{high}) in the livers of both genotypes. There were more Ly6C^{high}/CD11b^{high}/F4/80^{low} cells in *Ramp1*$^{-/-}$ mice than in WT mice, but fewer Ly6C^{high}/CD11b^{high}/F4/80^{high} cells (Fig 1D). These observations were associated with higher hepatic levels of chemokines, including C-C motif chemokine ligand 2 (*Ccl2*), *Ccl5*, and *Ccl7*, in *Ramp1*$^{-/-}$ mice than in WT mice (S3 Fig). By contrast, KCs (defined as Ly6C^{low}/CD11b^{low}/F4/80^{high}) were markedly reduced in both genotypes (Fig 1D). There were more CD4+ T cells (CD3^{high}/CD4^{high}/CD8^{low}) in the liver of *Ramp1*$^{-/-}$ mice than in that of WT mice (Fig. 1D). However, there were no significant differences between the genotypes in terms of the number of CD8+ T cells (CD3^{high}/CD4^{low}/CD8^{high}) in the liver (Fig 1D). These results suggest that RAMP1 protects the liver from ConA hepatotoxicity by inhibiting accumulation of inflammatory cells.

There were more monocytes (Ly6C^{high}/CD11b^{high}/F4/80^{low}) in the spleen of *Ramp1*$^{-/-}$ mice than in WT mice, but fewer macrophages (Ly6C^{high}/CD11b^{high}/F4/80^{high}) (Fig 1E). However, the percentage of these cells was small in both genotypes. There was a very small increase in the number of resident macrophages (Ly6C^{low}/CD11b^{low}/F4/80^{high}) in *Ramp1*$^{-/-}$ mice, along with moderate increases in the number of CD4+ T cells. By contrast, the number of CD8+ T cells fell in both genotypes (Fig 1E).

Expression of CGRP and RAMP1 during ConA-induced hepatitis

Next, we examined expression of RAMP1 in the liver and spleen from WT mice to investigate the potential role of RAMP1 in ConA-induced liver injury. Real-time PCR analysis revealed that the amount of *Ramp1* mRNA in the liver increased transiently at 1 h after ConA administration before declining thereafter, reaching a nadir at 6 h, and recovering to baseline levels at 24 h (S4 Fig). A gradual downregulation of *Ramp1* expression over time was observed in the spleen after ConA treatment (S4 Fig). A similar trend was observed for *Calcrl*, another subunit of the CGRP receptor, in the liver and spleen after ConA administration S4 Fig); however, the levels of *Calcrl* did not differ between *Ramp1*$^{-/-}$ and WT mice. Next, we tried to identify the cellular sources

of RAMP1. CGRP, a ligand of RAMP1, was also identified in nerve fibers within the liver and spleen (S4 Fig). CGRP levels fell over time after ConA treatment, and hepatic levels at 3, 6, and 24 h in *Ramp1*$^{-/-}$ mice were lower than those in WT mice (S4 Fig). CGRP expression in the spleen of both genotypes dropped at 1 h, before gradually returning to normal levels (S4 Fig); however, there were no significant differences between the genotypes. These results suggest that downregulation of CGRP/RAMP1 is associated with ConA hepatitis, and that RAMP1 in macrophages and T cells might play an important role in this process.

Increased expression of pro-inflammatory cytokines in *Ramp1*$^{-/-}$ mice with ConA hepatitis

Because pro-inflammatory cytokines, including TNFα and IFNγ, contribute to ConA hepatitis, we next measured *Tnf* and *Ifng* mRNA in the liver and spleen of mice with ConA hepatitis. Real-time PCR analysis revealed that WT and *Ramp1*$^{-/-}$ mice showed maximum expression of *Tnf* and *Ifng* at 1 h after ConA administration (Fig 2A). *Ramp1*$^{-/-}$ mice showed higher expression of *Tnf* and *Ifng* in the liver than WT mice. After 1 h, the levels of both cytokines fell. *Tnf* and *Ifng* mRNA expression was also higher in the spleen of *Ramp1*$^{-/-}$ mice (Fig 2B) than in that of WT mice, indicating that

Ramp1 signaling regulates expression of cytokines in the spleen, thereby contributing to ConA hepatitis.

Splenocytes play a role in ConA hepatitis

To investigate the possible role of splenocytes in development of ConA hepatitis, mice were subjected to splenectomy or a sham operation immediately prior to administration of ConA. At 6 h post-administration, the levels of ALT in splenectomized WT and *Ramp1*$^{-/-}$ mice decreased by 95% and 80%, respectively (Fig 3A). Thus, splenectomy ameliorated liver injury (as measured by ALT levels) in WT and *Ramp1*$^{-/-}$ mice. The mRNA levels of *Tnf* at 1 h after ConA treatment were decreased in splenectomized *Ramp1*$^{-/-}$ mice, but not splenectomized WT mice (Fig 3B). The mRNA levels of *Ifng* were downregulated in splenectomized WT and *Ramp1*$^{-/-}$ mice (Fig 3B). These results indicate that splenectomy suppresses the early phase of ConA hepatitis and that the spleen is the source of cytokines during ConA hepatitis.

To better understand which cells are responsible for producing pro-inflammatory cytokines in the spleen, we measured cytokine production by splenic macrophages and T cells. Flow cytometry analysis revealed that the numbers of TNFα- and IFNγ-producing F4/80+ macrophages in *Ramp1*$^{-/-}$ mice at 1 h post-ConA administration

were higher than in WT mice (Fig 4A). The numbers of TNFα- and IFNγ-producing CD4+ T cells in *Ramp1*$^{-/-}$ mice were also higher than those in WT mice (Fig 4B). These results indicate that RAMP1 signaling in splenic macrophages and T cells inhibits generation of TNFα and IFNγ in response to ConA. In addition, more CD4+ T cells than macrophages expressed these cytokines, suggesting that CD4+ T cells are the main source of TNFα and IFNγ during ConA hepatitis.

To better understand the role of RAMP1 signaling in splenic macrophages and CD4+ T cells, we isolated these cells from WT and *Ramp1*$^{-/-}$ mice and cultured them. Upon stimulation with ConA, CGRP downregulated *Tnf* and *Ifng* in splenic macrophages from WT mice, but upregulated them in splenic macrophages from *Ramp1*$^{-/-}$ mice (Fig 4C). Similarly, levels of *Tnf* and *Ifng* in splenic CD4+ T cells from WT mice were reduced, while those in splenic T cells from *Ramp1*$^{-/-}$ mice increased (Fig 4D). These results suggest that RAMP1 signaling in splenic macrophages and T cells downregulates expression of mRNA encoding *Tnf* and *Ifng*.

Splenectomy failed to reduce ALT levels in WT mice at 24 h after administration of ConA. By contrast, splenectomy decreased ALT levels in *Ramp1*$^{-/-}$ mice by 50% (see Fig 3A). At 6 h after ConA administration, splenectomy protected against ConA hepatitis in WT mice during the early phase, but not the late phase, of injury. Regarding

RAMP1 signaling, splenectomy led to a partial improvement in ConA hepatitis in *Ramp1*$^{-/-}$ mice, suggesting that RAMP1 signaling in splenocytes participates in ConA-mediated hepatitis. Taken together, the results suggest that RAMP1-expressing cells other than splenocytes are required for amplification of liver injury elicited by ConA.

To further clarify the role of T cells (CD4+ cells) in ConA hepatitis, we treated WT and *Ramp1*$^{-/-}$ mice with an anti-CD4 antibody 24 h before ConA treatment. The anti-CD4 antibody suppressed ConA liver injury in WT and *Ramp1*$^{-/-}$ mice at 6 and 24 h post-ConA administration. The anti-CD4 antibody caused a partial reduction in ALT levels, suggesting that RAMP1 signaling in CD4+ T cells makes a limited contribution to ConA hepatitis (Fig 4E). These results were consistent with those observed in mice subjected to splenectomy.

To elucidate the contribution of RAMP1 signaling in splenic T cells to ConA hepatitis, we isolated splenic CD4+ T cells from *Ramp1*$^{-/-}$ mice and adoptively transferred them into WT mice. Transfer of *Ramp1*-deficient CD4+ T cells increased ALT levels (Fig 4F). However, the magnitude of liver injury in WT mice receiving *Ramp1*-deficient CD4+ T cells was lower than that in *Ramp1* null mice, suggesting that *Ramp1*-deficient CD4+ T cells play a role (at least partially) in exacerbating liver injury in global

knockout *Ramp1* mice. Conversely, *Ramp1*-deficient cells other than splenic CD4+ T cells exacerbate ConA hepatitis in *Ramp1*$^{-/-}$ mice.

RAMP1 in KCs protects the liver from ConA hepatitis

Next, we examined whether hepatic macrophages aggravate ConA hepatitis in *Ramp1*$^{-/-}$ mice. In agreement with previous studies, we found that pre-treatment with clodronate liposomes (CL) attenuated ConA hepatitis in WT and *Ramp1*$^{-/-}$ mice (Fig 5A and 5B), suggesting that KCs are involved in induction and progression of ConA hepatitis. Treatment with CL also reduced *Tnf* and *Ifng* expression in WT (Fig 5C and 5E) and *Ramp1*$^{-/-}$ (Fig 5D and 5F) mice. At 24 h post-ConA treatment, CL suppressed accumulation of inflammatory cells (CD68+ and Ly6C+ cells) in WT and *Ramp1*$^{-/-}$ mice (S5 Fig), which was associated with downregulation of chemokines (*Ccl2* and *Ccl7*) (S5 Fig). These results suggest that RAMP1 signaling in KCs is responsible for ConA-mediated hepatitis.

TNFα and IFNγ are key causative agents of ConA hepatitis. To elucidate the role of TNFα/IFNγ in our model, WT mice were treated with neutralizing anti-TNFα and anti-IFNγ antibodies prior to ConA administration. Blocking TNFα/IFNγ prevented ConA-induced liver injury, as evidenced by reduced ALT levels, less hepatic necrosis,

452 and reduced infiltration of the liver by monocytes/macrophages and T cells (S6 Fig).
453 These results indicate that TNFα/IFNγ play a critical role in mediating ConA-induced
454 hepatitis.

455 Next, we measured TNFα and IFNγ secreted by hepatic macrophages and T cells using
456 flow cytometry analysis. At 1 h after ConA treatment, the number of TNFα-expressing
457 KCs in *Ramp1*$^{-/-}$ mice was higher than that in WT mice (Fig 6A). By contrast, there was
458 no significant difference in the number of TNFα-expressing CD4+ T cells between the
459 genotypes. The number of IFNγ-expressing KCs in *Ramp1*$^{-/-}$ mice was also greater than
460 that in WT mice (Fig 6B). However, no significant difference in the number of
461 IFNγ-expressing CD4+ T cells between the genotypes was observed. These results
462 suggest that, in the liver, RAMP1 signaling downregulates cytokine production by KCs.

463 Because RAMP1 signaling in KCs appears to be involved in ConA hepatitis, we next
464 isolated KCs and treated them with CGRP. We found that expression of mRNA
465 encoding *Tnf* and *Ifng* in *Ramp1*-deficient KCs stimulated with CGRP (10 nM) was
466 enhanced when compared with that in WT KCs (Fig 6C).

467 To further examine the interaction between KCs and T cells, we co-cultured isolated
468 KCs (F4/80+ cells) and splenic T cells (CD4+ cells) isolated from WT and *Ramp1*$^{-/-}$
469 mice. Stimulating co-cultured KCs and splenic T cells with ConA further upregulated

expression of *Tnf* and *Ifng* when compared with cultured KCs alone or splenic T cells alone (Fig 6D). CGRP reversed the increase in cytokine expression by co-cultured cells from WT mice, but not those from *Ramp1*$^{-/-}$ mice (Fig 6D). These results suggest that the interaction between splenic T cells and KCs contributes to ConA hepatitis, which is dependent on RAMP1.

CGRP suppresses ALT and cytokine production in mice with ConA hepatitis

Finally, to examine whether CGRP suppresses hepatic inflammation elicited by ConA, we investigated the effect of CGRP administration on ALT and cytokine levels. As shown in Fig 7, CGRP administration reduced ALT levels at 24 h; it also reduced expression of mRNA encoding *Tnf* and *Ifng* in the liver and spleen at 1 h.

Discussion

Sensory neurons communicate actively with the immune system. Here, we demonstrated that RAMP1 signaling plays an immunosuppressive role in ConA-mediated hepatitis by downregulating production of pro-inflammatory cytokines

488 by KCs and splenic T cells. Both T cells and macrophages play key roles in
489 ConA-mediated hepatitis by producing TNFα and IFNγ, both of which cause liver
490 injury. Our data show that splenic T cells trigger hepatic inflammatory responses to
491 ConA and interact with KCs to induce liver injury. KCs are essential for induction and
492 amplification of ConA-mediated hepatitis. RAMP1 signaling inhibits development of
493 ConA-induced hepatitis by inactivating hepatic and splenic immune cells. These
494 findings indicate that RAMP1 is a good therapeutic target for immune-mediated
495 hepatitis.

496 Although the roles of sensory neuron-immune interactions in response to sterile tissue
497 damage are not fully understood, we showed previously that RAMP1 signaling
498 regulates inflammation by suppressing inflammatory mediators released from immune
499 cells such as dendritic cells, macrophages, and lymphocytes [9,10]. CGRP also
500 contributes to wound healing and secondary lymphedema by affecting RAMP1
501 signaling in macrophages [21,22]. These findings indicate that CGRP secreted from
502 endings of sensory nerve fibers regulates immune function via RAMP1 signaling.

503 ConA-induced liver injury is a model for immune-mediated hepatitis, a condition that
504 causes T cell activation followed by increased expression of inflammatory cytokines.
505 During this process, CD4+ T cell-mediated activation of macrophages is a crucial

pathogenic parameter [12]. In the liver, endogenous CGRP protects against ConA-induced liver injury [11]. Indeed, *Calca*-deficient (*Calca*$^{-/-}$) mice exhibit aggravation of ConA hepatitis upon reduction of the hepatotrophic cytokine IL-6 and increased apoptosis [11]. However, the role of CGRP receptors in immune-mediated hepatitis is unclear. Here, we demonstrate that RAMP1 attenuates ConA-mediated hepatitis.

CGRP acts on immune cells directly and regulates their production of cytokines in inflammatory lesions [23]. Previously, we reported that RAMP1 is expressed by T cells [10,24], dendritic cells [9], and macrophages [21,22], and that RAMP1 expression by these immune cells is essential for development of inflammation during endotoxemia and colitis. Here, we show that RAMP1 is expressed by hepatic and splenic macrophages and by splenic T cells. These results suggest that immune cells in the liver and spleen are major sites of RAMP1 expression during ConA hepatitis. CGRP and its receptor are expressed in various organs, including liver [15] and spleen [16,17]. In addition, we show that CGRP levels in the liver and spleen fell upon exposure to ConA, and that *Ramp1*$^{-/-}$ mice express less CGRP than WT mice. Although CGRP is easily degraded by proteinases present in the circulation immediately after release, maintaining CGRP levels is important for preventing liver injury. Indeed, the data

524 demonstrate that supplementation with CGRP effectively attenuated Con A hepatitis via
525 suppression of pro-inflammatory cytokines.

526 The spleen is considered a source of pro-inflammatory mediators capable of
527 propagating injury. Accumulating evidence suggests that stimulating the vagus nerve
528 reduces cytokine production by splenic macrophages [25,26]. Binding of the cholinergic
529 receptor (expressed by splenic macrophages) is required for vagus nerve-mediated
530 inhibition of TNFα release [25]. These findings indicate that immune cells and neurons
531 share common signaling molecules, and that the nervous system limits excessive
532 immune activity. Regarding sensory innervation of the spleen, CGRP+ nerve terminals
533 are sited close to the zones in which macrophages and T cells are situated [4]. Therefore,
534 it is important to understand the role of sensory neural innervation of the spleen when
535 examining immune-mediated regulation of tissue injury. The spleen is influenced by, or
536 involved in, the pathophysiology of ConA hepatitis. ConA triggers proliferation of and
537 cytokine production by splenic lymphocytes; activated splenic T cells then migrate to
538 the liver to aggravate liver injury [12,27]. The present study shows that splenectomy
539 immediately prior to ConA administration attenuates ConA hepatitis by reducing
540 secretion of pro-inflammatory cytokines. Therefore, the spleen contributes to the early
541 phase of ConA hepatitis by producing pro-inflammatory mediators. However,

542 splenectomy in WT mice did not attenuate ConA hepatitis at 24 h, suggesting that the
543 spleen by itself is not responsible for the severity of the disease. Consistent with this,
544 splenectomy 2 weeks before ConA treatment did not affect liver injury induced by
545 ConA treatment [28]. However, ALT levels in splenectomized *Ramp1*$^{-/-}$ mice fell by
546 50% at 24 h after ConA treatment when compared with those in sham-operated *Ramp1*$^{-/-}$
547 mice, suggesting that RAMP1 signaling in splenocytes improves ConA-mediated
548 hepatitis.

549 The data also indicate that production of TNFα and IFNγ by activated splenic CD4+ T
550 cells in *Ramp1*$^{-/-}$ mice was inhibited from as early as 1 h after ConA treatment, at which
551 time no significant liver injury was seen. These results suggest that splenic T cells
552 contribute to ConA hepatitis by producing TNFα and IFNγ, which is dependent on
553 RAMP1 signaling. Alternatively, the spleen (in which T cells are dysregulated after loss
554 of RAMP1-mediated signaling) is the induction site for ConA hepatitis.

555 We evaluated whether CD4+ T cells are required for ConA hepatitis. Treatment with
556 an anti-CD4 antibody attenuated, but only partly, ConA-mediated hepatitis, indicating
557 that activated CD4+ T cells are responsible for the disease progression. To further
558 determine whether RAMP1 signaling in splenic CD4+ T cells plays a role in
559 development of ConA hepatitis, we examined the effect of adoptively transferring

splenic CD4+ T cells from *Ramp1*$^{-/-}$ mice. Transfer of *Ramp1*-deficient splenic CD4+ T cells led to a modest increase in liver injury compared with that in global *Ramp1*-deficient mice. These results suggest that RAMP1 signaling in splenic CD4+ T cells participates in ConA-mediated hepatitis.

In addition to that in splenic T cells, we found that RAMP1 signaling in splenic macrophages suppressed production of TNFα and IFNγ. However, splenic macrophages produced fewer pro-inflammatory cytokines than splenic T cells; indeed, flow cytometry analysis revealed that the population of cytokine-secreting cells within splenic macrophages was smaller than that within splenic T cells.

ConA-induced liver injury is initiated not only by specific activation of CD4+ lymphocytes, but also by KCs [13]. Eliminating macrophages markedly attenuates ConA hepatitis [13,14], suggesting that KCs are involved in ConA hepatitis. Consistent with this, we found that deleting macrophages using CL reduced the severity of ConA hepatitis associated with pro-inflammatory mediators in WT and *Ramp1*$^{-/-}$ mice. In addition, flow cytometry analysis and *in vitro* studies revealed that RAMP1 signaling downregulated secretion of pro-inflammatory cytokines by KCs. Therefore, production of pro-inflammatory cytokines by KCs is RAMP1-dependent, and RAMP1 signaling in KCs is important for development of ConA hepatitis.

578 Although macrophage deletion reduced the severity of ConA hepatitis, it also partially
579 suppressed production of pro-inflammatory cytokines. This indicated that cells other
580 than KCs are the source of inflammatory cytokines after ConA stimulation. During the
581 early phase of ConA hepatitis, we detected modest infiltration by hepatic T cells and
582 moderate increases in the number of hepatic CD4+ T cells expressing TNFα and IFNγ
583 in both genotypes, suggesting that RAMP1 signaling in hepatic T cells plays a minor
584 role in early liver injury elicited by ConA. Instead, splenic CD4 T cells, in addition to
585 KCs, were activated as early as 1 h after ConA administration, as evidenced by
586 increased cytokine production, indicating that ConA activates splenic T cells and KCs
587 simultaneously. Furthermore, despite the presence of persistently activated CD4+ T
588 cells in mice treated with CL, the liver was protected from ConA hepatitis, indicating
589 that KCs are required for continuous progression of ConA hepatitis.
590 After simultaneous activation of splenic T cells and KCs during the course of
591 ConA-mediated hepatitis, migrated splenic T cells induce liver injury by interacting
592 with KCs. This interaction was suggested by results from co-cultures of isolated KCs
593 and splenic T cells. The data showed that expression of pro-inflammatory cytokines in
594 co-culture systems was higher than that in individual cell cultures, and that exacerbated
595 KC and splenic T cell responses to ConA were dependent on RAMP1. Our data also

support the notion that TNFα and IFNγ are critical for induction of ConA hepatitis; indeed, we found that antibodies specific for TNFα and IFNγ attenuated ConA hepatitis and liver infiltration by inflammatory cells.

Although KCs are crucial for development of ConA hepatitis, their numbers fell significantly at 24 h after ConA treatment. KC-generated cytokines recruited Ly6C- or CD68-positive monocytes/macrophages, leading to extensive liver injury during the late phase of ConA hepatitis. Of interest, the liver of WT mice was infiltrated by $Ly6C^{high}/CD11b^{high}/F4/80^{high}$ cells, while that of *Ramp1*$^{-/-}$ mice displayed accumulation of $Ly6C^{high}/CD11b^{high}/F4/80^{low}$ cells. This suggests that susceptibility of *Ramp1*$^{-/-}$ mice to ConA hepatitis is related to alterations in macrophage phenotype. Preliminary studies showed that the survival rate of WT mice with ConA hepatitis was 100%, and that ALT levels at 48 h were 206 ± 40 IU/L (n = 6). By contrast, survival rates for *Ramp1*$^{-/-}$ mice were significantly lower. Considering the different mortality rates and mechanisms of liver injury between the two genotypes, it may be that $Ly6C^{high}/CD11b^{high}/F4/80^{high}$ monocyte-derived macrophages in WT mice contribute to resolution of inflammation after ConA hepatitis, while $Ly6C^{high}/CD11b^{high}/F4/80^{low}$ monocyte-derived macrophages in *Ramp1*$^{-/-}$ mice exacerbate inflammation in response to ConA. Indeed, $Ly6C^{high}/CD11b^{high}/F4/80^{high}$ monocyte-derived macrophages are involved in liver

repair after acetaminophen hepatotoxicity [29]. In addition, we recently reported that Ly6C^{high}/CD11b^{high}/F4/80^{low} cells recruited to the liver display a pro-inflammatory macrophage phenotype and delay liver repair after hepatic ischemia/reperfusion [20]. The phenotypes of macrophages recruited to injured livers at 24 h post-ConA treatment were different in WT and *Ramp1*$^{-/-}$ mice, indicating that RAMP1 signaling is involved in macrophage polarization. Further studies are needed to elucidate the role of RAMP1 signaling in resolution of liver inflammation and liver repair during ConA hepatitis.

In conclusion, the present study demonstrates that RAMP1 signaling in KCs plays a crucial role in preventing and/or limiting immune-mediated hepatitis; this may have important implications for the treatment of patients with autoimmune liver inflammation. Considering that dysregulation of RAMP1 function has marked effects on the outcome of murine liver inflammation, selective agonists of RAMP1 might be a therapeutic option for immune-mediated hepatitis. Therefore, restorative therapies aiming at restoring RAMP1 activity in the immune cells might modulate liver injury.

Acknowledgements

We thank Michiko Ogino and Kyoko Yoshikawa for their technical assistance.

References

1. Heymann F, Tacke F. Immunology in the liver--from homeostasis to disease. Nat Rev Gastroenterol Hepatol. 2016 Feb;13(2):88-110. doi: 10.1038/nrgastro.2015.200. Epub 2016 Jan 13. Review. PubMed PMID: 26758786.

2. Jensen KJ, Alpini G, Glaser S. Hepatic nervous system and neurobiology of the liver. Compr Physiol. 2013 Apr;3(2):655-65. doi: 10.1002/cphy.c120018. Review. PubMed PMID: 23720325; PubMed Central PMCID: PMC3733049.

3. Stoyanova II, Gulubova MV. Immunocytochemical study on the liver innervation in patients with cirrhosis. Acta Histochem. 2000 Nov;102(4):391-402. PubMed PMID: 11145532.

4. Jung WC, Levesque JP, Ruitenberg MJ. It takes nerve to fight back: The significance of neural innervation of the bone marrow and spleen for immune function. Semin Cell Dev Biol. 2017 Jan;61:60-70. doi: 10.1016/j.semcdb.2016.08.010. Epub 2016 Aug 11. Review. PubMed PMID: 27523920.

650

651 5. Poyner DR, Sexton PM, Marshall I, Smith DM, Quirion R, Born W, et al.
652 International Union of Pharmacology. XXXII. The mammalian calcitonin gene-related
653 peptides, adrenomedullin, amylin, and calcitonin receptors. Pharmacol Rev. 2002
654 Jun;54(2):233-46. Review. PubMed PMID: 12037140.

655

656 6. Hay DL, Poyner DR, Quirion R; International Union of Pharmacology. International
657 Union of Pharmacology. LXIX. Status of the calcitonin gene-related peptide subtype
658 2 receptor. Pharmacol Rev. 2008 Jun;60(2):143-5. doi: 10.1124/pr.108.00372. Epub
659 2008 Jun 13. PubMed PMID: 18552275.

660

661 7. McLatchie LM, Fraser NJ, Main MJ, Wise A, Brown J, Thompson N, et al. RAMPs
662 regulate the transport and ligand specificity of the calcitonin-receptor-like receptor.
663 Nature. 1998 May 28;393(6683):333-9. PubMed PMID: 9620797.

664

665 8. Miyauchi K, Tadotsu N, Hayashi T, Ono Y, Tokoyoda K, Tsujikawa K, et al.
666 Molecular cloning and characterization of mouse calcitonin gene-related peptide
667 receptor. Neuropeptides. 2002 Feb;36(1):22-33. PubMed PMID: 12147211.

9. Tsujikawa K, Yayama K, Hayashi T, Matsushita H, Yamaguchi T, Shigeno T, et al. Hypertension and dysregulated proinflammatory cytokine production in receptor activity-modifying protein 1-deficient mice. Proc Natl Acad Sci U S A. 2007 Oct 16;104(42):16702-7. Epub 2007 Oct 8. PubMed PMID: 17923674; PubMed Central PMCID: PMC2034234.

10. Kawashima-Takeda N, Ito Y, Nishizawa N, Kawashima R, Tanaka K, Tsujikawa K, et al. RAMP1 suppresses mucosal injury from dextran sodium sulfate-induced colitis in mice. J Gastroenterol Hepatol. 2017 Apr;32(4):809-818. doi: 10.1111/jgh.13505. PubMed PMID: 27513455.

11. Kamiyoshi A, Sakurai T, Ichikawa-Shindo Y, Fukuchi J, Kawate H, Muto S, et al. Endogenous alphaCGRP protects against concanavalin A-induced hepatitis in mice. Biochem Biophys Res Commun. 2006 Apr 28;343(1):152-8. Epub 2006 Mar 3. PubMed PMID: 16530166.

12. Tiegs G, Hentschel J, Wendel A. A T cell-dependent experimental liver injury in

686 mice inducible by concanavalin A. J Clin Invest. 1992 Jul;90(1):196-203. PubMed
687 PMID: 1634608; PubMed Central PMCID: PMC443081.
688
689 13. Schümann J, Wolf D, Pahl A, Brune K, Papadopoulos T, van Rooijen N, et al.
690 Importance of Kupffer cells for T-cell-dependent liver injury in mice. Am J Pathol.
691 2000 Nov;157(5):1671-83. PubMed PMID: 11073826; PubMed Central PMCID:
692 PMC1885735.
693
694 14. Nakashima H, Kinoshita M, Nakashima M, Habu Y, Shono S, Uchida T, et al.
695 Superoxide produced by Kupffer cells is an essential effector in concanavalin
696 A-induced hepatitis in mice. Hepatology. 2008 Dec;48(6):1979-88. doi:
697 10.1002/hep.22561. PubMed PMID: 18942689.
698
699 15. Kroeger I, Erhardt A, Abt D, Fischer M, Biburger M, Rau T, et al. The neuropeptide
700 calcitonin gene-related peptide (CGRP) prevents inflammatory liver injury in mice. J
701 Hepatol. 2009 Aug;51(2):342-53. doi: 10.1016/j.jhep.2009.03.022. Epub 2009 May 3.
702 PubMed PMID: 19464067.
703

16. Rosenfeld MG, Emeson RB, Yeakley JM, Merillat N, Hedjran F, Lenz J, et al. Calcitonin gene-related peptide: a neuropeptide generated as a consequence of tissue-specific, developmentally regulated alternative RNA processing events. Ann N Y Acad Sci. 1992 Jun 30;657:1-17. Review. PubMed PMID: 1637077.

17. Bulloch K, McEwen BS, Nordberg J, Diwa A, Baird S. Selective regulation of T-cell development and function by calcitonin gene-related peptide in thymus and spleen. An example of differential regional regulation of immunity by the neuroendocrine system. Ann N Y Acad Sci. 1998 May 1;840:551-62. PubMed PMID: 9629282.

18. Fujita T, Soontrapa K, Ito Y, Iwaisako K, Moniaga CS, Asagiri M, et al. Hepatic stellate cells relay inflammation signaling from sinusoids to parenchyma in mouse models of immune-mediated hepatitis. Hepatology. 2016 Apr;63(4):1325-39. doi: 10.1002/hep.28112. Epub 2015 Sep 30. PubMed PMID: 26248612.

19. Kojo K, Ito Y, Eshima K, Nishizawa N, Ohkubo H, Yokomizo T, et al. BLT1 signalling protects the liver against acetaminophen hepatotoxicity by preventing

722 excessive accumulation of hepatic neutrophils. Sci Rep. 2016 Jul 11;6:29650. doi:
723 10.1038/srep29650. PubMed PMID: 27404729; PubMed Central PMCID:
724 PMC4939602.

725

726 20. Nishizawa N, Ito Y, Eshima K, Ohkubo H, Kojo K, Inoue T, et al. Inhibition of
727 microsomal prostaglandin E synthase-1 facilitates liver repair after hepatic injury in
728 mice. J Hepatol. 2018 Feb 16. pii: S0168-8278(18)30126-0. doi:
729 10.1016/j.jhep.2018.02.009. [Epub ahead of print] PubMed PMID: 29458169.

730

731 21. Kurashige C, Hosono K, Matsuda H, Tsujikawa K, Okamoto H, Majima M. Roles
732 of receptor activity-modifying protein 1 in angiogenesis and lymphangiogenesis during
733 skin wound healing in mice. FASEB J. 2014 Mar;28(3):1237-47. doi:
734 10.1096/fj.13-238998. Epub 2013 Dec 5. PubMed PMID: 24308973.

735

736 22. Mishima T, Ito Y, Nishizawa N, Amano H, Tsujikawa K, Miyaji K, et al. RAMP1
737 signaling improves lymphedema and promotes lymphangiogenesis in mice. J Surg Res.
738 2017 Nov;219:50-60. doi: 10.1016/j.jss.2017.05.124. Epub 2017 Jun 23. PubMed
739 PMID: 29078910.

740

741 23. Holzmann B. Antiinflammatory activities of CGRP modulating innate immune
742 responses in health and disease. Curr Protein Pept Sci. 2013 Jun;14(4):268-74. Review.
743 PubMed PMID: 23745695.

744

745 24. Mikami N, Matsushita H, Kato T, Kawasaki R, Sawazaki T, Kishimoto T, et al.
746 Calcitonin gene-related peptide is an important regulator of cutaneous immunity: effect
747 on dendritic cell and T cell functions. J Immunol. 2011 Jun 15;186(12):6886-93. doi:
748 10.4049/jimmunol.1100028. Epub 2011 May 6. PubMed PMID: 21551361.

749

750 25. Wang H, Yu M, Ochani M, Amella CA, Tanovic M, Susarla S, et al. Nicotinic
751 acetylcholine receptor alpha7 subunit is an essential regulator of inflammation. Nature.
752 2003 Jan 23;421(6921):384-8. Epub 2002 Dec 22. PubMed PMID: 12508119.

753

754 26. Rosas-Ballina M, Olofsson PS, Ochani M, Valdés-Ferrer SI, Levine YA, Reardon C,
755 et al. Acetylcholine-synthesizing T cells relay neural signals in a vagus nerve circuit.
756 Science. 2011 Oct 7;334(6052):98-101. doi: 10.1126/science.1209985. Epub 2011 Sep
757 15. PubMed PMID: 21921156; PubMed Central PMCID: PMC4548937.

27. Bonder CS, Ajuebor MN, Zbytnuik LD, Kubes P, Swain MG. Essential role for neutrophil recruitment to the liver in concanavalin A-induced hepatitis. J Immunol. 2004 Jan 1;172(1):45-53. PubMed PMID: 14688308.

28. Amiya T, Nakamoto N, Chu PS, Teratani T, Nakajima H, Fukuchi Y, et al. Bone marrow-derived macrophages distinct from tissue-resident macrophages play a pivotal role in Concanavalin A-induced murine liver injury via CCR9 axis. Sci Rep. 2016 Oct 11;6:35146. doi: 10.1038/srep35146. PubMed PMID: 27725760; PubMed Central PMCID: PMC5057133.

29. Zigmond E, Samia-Grinberg S, Pasmanik-Chor M, Brazowski E, Shibolet O, Halpern Z, et al. Infiltrating monocyte-derived macrophages and resident kupffer cells display different ontogeny and functions in acute liver injury. J Immunol. 2014 Jul 1;193(1):344-53. doi: 10.4049/jimmunol.1400574. Epub 2014 Jun 2. PubMed PMID: 24890723.

Figure legends

Fig 1. Deficient RAMP1 signaling exacerbates ConA-induced liver injury via infiltration of inflammatory cells into the liver.

Ramp1$^{-/-}$ and WT mice were administered ConA (20 mg/kg) by intraperitoneal (i.p.) injection. (a) Kaplan-Meier survival curves for *Ramp1*$^{-/-}$ mice (n = 20) and WT mice (n = 20) at various time points after receiving ConA. Survival data analyzed by log-rank test *p < 0.05 *vs.* WT mice. (b) Serum levels of ALT and the area of hepatic necrosis (expressed as a percentage) after ConA administration. Data are expressed as the mean ± SD (n = 6 mice per group). *p < 0.05 *vs.* WT mice. Serum samples at 0, 1, 3, 6, and 24 h after ConA administration were collected, and ALT levels were measured. (c) Numbers of hepatic Ly6C+ cells, CD68+ cells, and CD4+ cells at 24 h after ConA administration. Data are expressed as the mean ± SD of six mice per group. *p < 0.05 *vs.* WT mice. (d, e) Flow cytometry analysis of the percentage of Ly6C^{high}/CD11b^{high}/F4/80^{low} cells, Ly6C^{high}/CD11b^{high}/F4/80^{high} cells Ly6C^{low}/CD11b^{low}/F4/80^{high} cells, CD3^{high}/CD4^{high}/CD8^{low} cells, and CD3^{high}/CD4^{low}/CD8^{high} cells within the CD45+ cell population in the liver (d) and spleen (e) at 0 and 24 h after ConA treatment. Data are expressed as the mean ± SD of six mice per group. *p < 0.05 *vs.* WT mice.

794

795 **Fig 2. Increased expression of pro-inflammatory cytokines in *Ramp1*$^{-/-}$ mice with**

796 **ConA hepatitis.**

797 Time course of changes in mRNA levels of *Tnf* and *Ifng* in the liver (a) and spleen (b)

798 of WT and *Ramp1*$^{-/-}$ mice after ConA treatment. Data are expressed as the mean ± SD

799 from six mice per group. *$p < 0.05$ *vs.* WT mice.

800

801 **Fig 3. Effects of splenectomy on ALT and pro-inflammatory cytokines levels in**

802 **mice with ConA hepatitis.**

803 (a) Splenectomy reduced ALT levels in WT and *Ramp1*$^{-/-}$ mice at 6 h (left) and 24 h

804 (right) after ConA treatment. ConA was administered immediately after splenectomy.

805 Data are expressed as the mean ± SD from 4–6 mice per group. *$p < 0.05$. (b) Effect of

806 splenectomy on *Tnf* and *Ifng* mRNA levels in liver from WT and *Ramp1*$^{-/-}$ mice at 1 h

807 after ConA administration. ConA was administered immediately after splenectomy.

808 Data are expressed as the mean ± SD from 4–6 mice per group. *$p < 0.05$.

809

810 **Fig 4. RAMP1 signaling regulates expression of pro-inflammatory cytokines by**

811 **splenic macrophages and T cells.**

812 (a, b) The numbers of TNFα- and IFNγ-expressing cells within splenic F4/80+ cells (a)
813 and splenic CD4+ T cells (b) populations from WT and *Ramp1*$^{-/-}$ mice at 1 h after ConA
814 treatment. Expression of TNFα and IFNγ was analyzed by flow cytometry. Data are
815 expressed as the mean ± SD from six mice per group. *p < 0.05 *vs.* WT mice. (c)
816 Amounts of *Tnf* and *Ifng* mRNA expressed by splenic F4/80+ cells isolated from WT
817 and *Ramp1*$^{-/-}$ mice. Isolated splenic macrophages were stimulated with CGRP (1 and 10
818 nM) with or without ConA for 3 h. Macrophages were isolated by magnetic-activated
819 cell sorting (MACS). Data are expressed as the mean ± SD from 4–5 mice per group. *p
820 < 0.05. (d) Expression of *Tnf* and *Ifng* mRNA by splenic CD4+ T cells isolated from
821 WT and *Ramp1*$^{-/-}$ mice. Isolated splenic CD4+ T cells were stimulated with CGRP with
822 or without ConA for 1 h. CD4+ T cells were isolated by magnetic-activated cell sorting
823 (MACS). Data are expressed as the mean ± SD from 4–5 mice per group. *p < 0.05.
824 (e) Serum ALT levels after deletion of CD4+ T cells from WT and *Ramp1*$^{-/-}$ mice during
825 ConA hepatitis. Anti-CD4 antibodies or isotype IgG was administered 24 h before
826 ConA treatment. Data are expressed as the mean ± SD from 3–6 mice per group. *p <
827 0.05 *vs.* IgG-treated mice. (f) Adoptive transfer of CD4+ T cells from *Ramp1*$^{-/-}$ mice
828 into WT mice (*Ramp1*$^{-/-}$→WT). Data are expressed as the mean ± SD from 3–6 mice
829 per group. *p < 0.05 *vs.* WT→WT.

Fig 5. Deleting macrophages attenuates ConA-induced liver injury and decreases production of pro-inflammatory cytokines.

(a, b) ALT levels in WT mice (a) and *Ramp1*$^{-/-}$ mice (b) treated with clodronate liposomes (CL). Mice were treated with CL or vehicle (PBS) 48 h before ConA administration. Data are expressed as the mean ± SD from 3–6 mice per group. *p < 0.05. (c–f) Amounts of *Tnf* mRNA in WT mice (c) and *Ramp1*$^{-/-}$ mice (d) treated with CL, and amounts of *Ifng* mRNA in WT mice (e) and *Ramp1*$^{-/-}$ mice (f) treated with CL. Data are expressed as the mean ± SD from 3–6 mice per group. *p < 0.05.

Fig 6. RAMP1 signaling regulates expression of pro-inflammatory cytokines in hepatic macrophages and splenic T cells.

(a, b) The numbers of TNFα- and IFNγ-producing F4/80+ cells (a) and the numbers of TNFα- and IFNγ-producing CD4+ T cells (b) in the liver from WT and *Ramp1*$^{-/-}$ mice at 1 h after ConA treatment. Expression of TNFα and IFNγ was analyzed by flow cytometry. Data are expressed as the mean ± SD from six mice per group. *p < 0.05 *vs.* WT mice. (c) Amounts of *Tnf* and *Ifng* mRNA in KCs isolated from WT and *Ramp1*$^{-/-}$ mice. Isolated KCs were stimulated with CGRP (1 and 10 nM) with or without ConA

for 3 h. KCs were isolated by magnetic-activated cell sorting (MACS). Data are expressed as the mean ± SD from 4–5 mice per group. *p < 0.05 *vs.* WT mice. (d) Amounts of *Tnf* and *Ifng* mRNA in KCs and/or splenic CD4+ T cells isolated from WT and *Ramp1*$^{-/-}$ mice. KCs co-cultured with splenic CD4+ T cells were stimulated with CGRP with or without ConA for 1 h. Data are expressed as the mean ± SD from 4–5 mice per group. *p < 0.05.

Fig 7. Effects of CGRP treatment on ALT and pro-inflammatory cytokine levels during ConA hepatitis.

CGRP or vehicle was administered 30 min before ConA treatment. (a) ALT levels in WT mice treated with CGRP at 1 h and 24 h after ConA administration. Veh, vehicle. Data are expressed as the mean ± SD from 4–6 mice per group. *p < 0.05. (b) Amount of *Tnf* mRNA in the liver and spleen after ConA administration. Data are expressed as the mean ± SD from 4–6 mice per group. *p < 0.05. (c) Amount of *Ifng* mRNA in liver and spleen after ConA administration. Data are expressed as the mean ± SD from 4–6 mice per group. *p < 0.05.

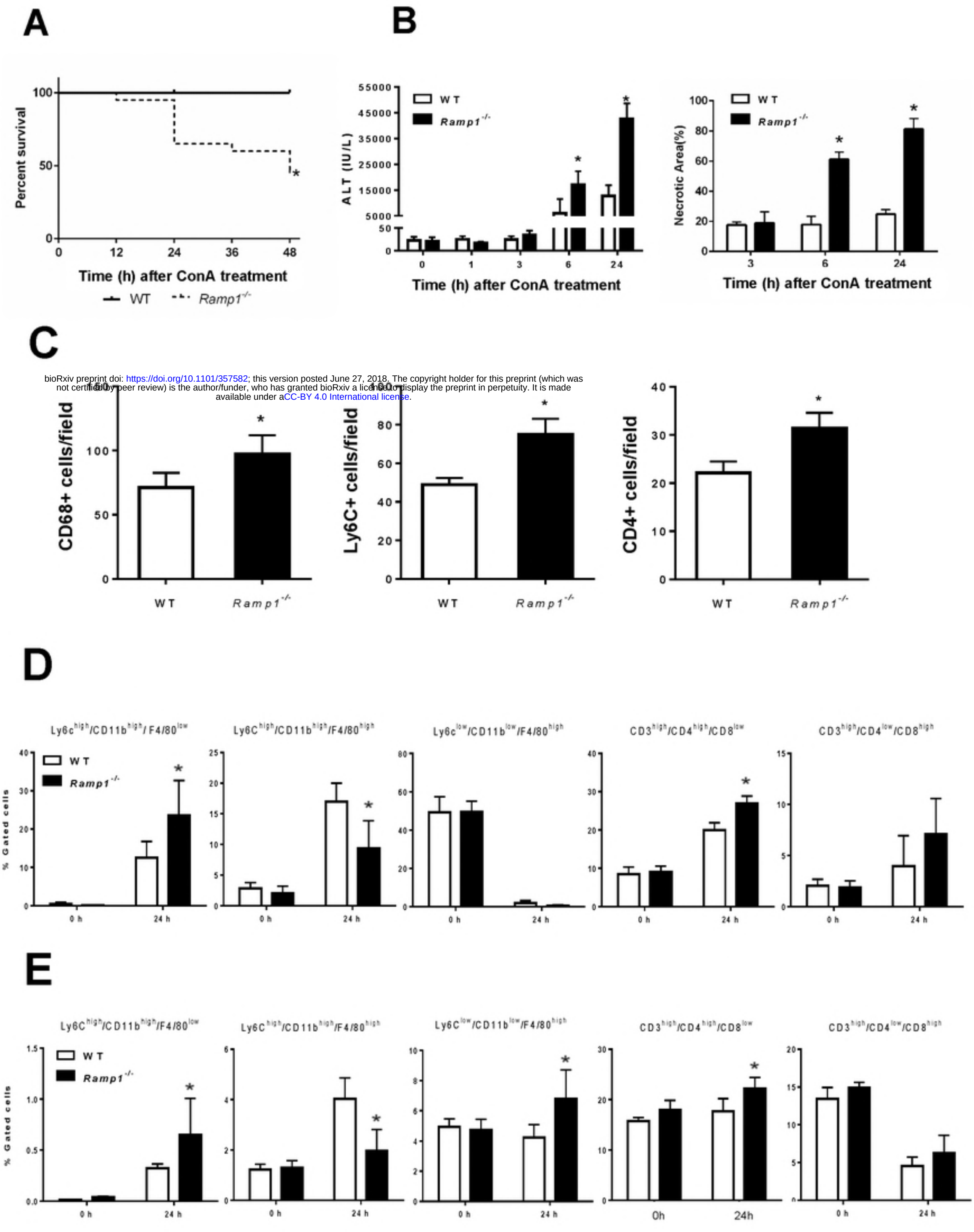

Fig 1

A

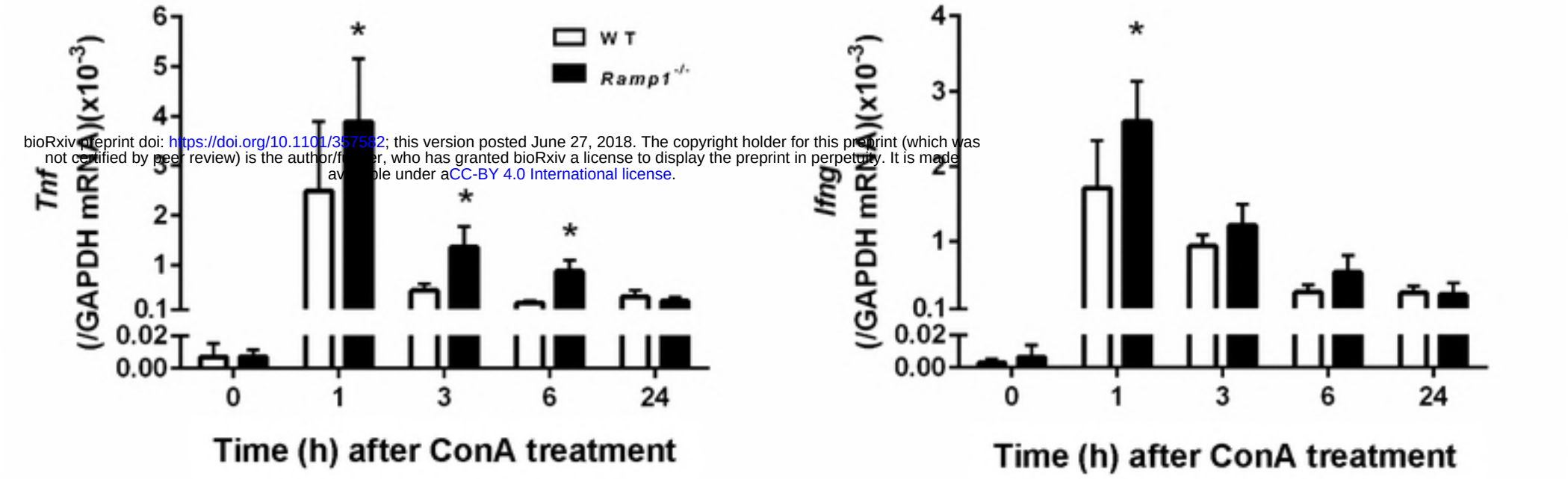

B

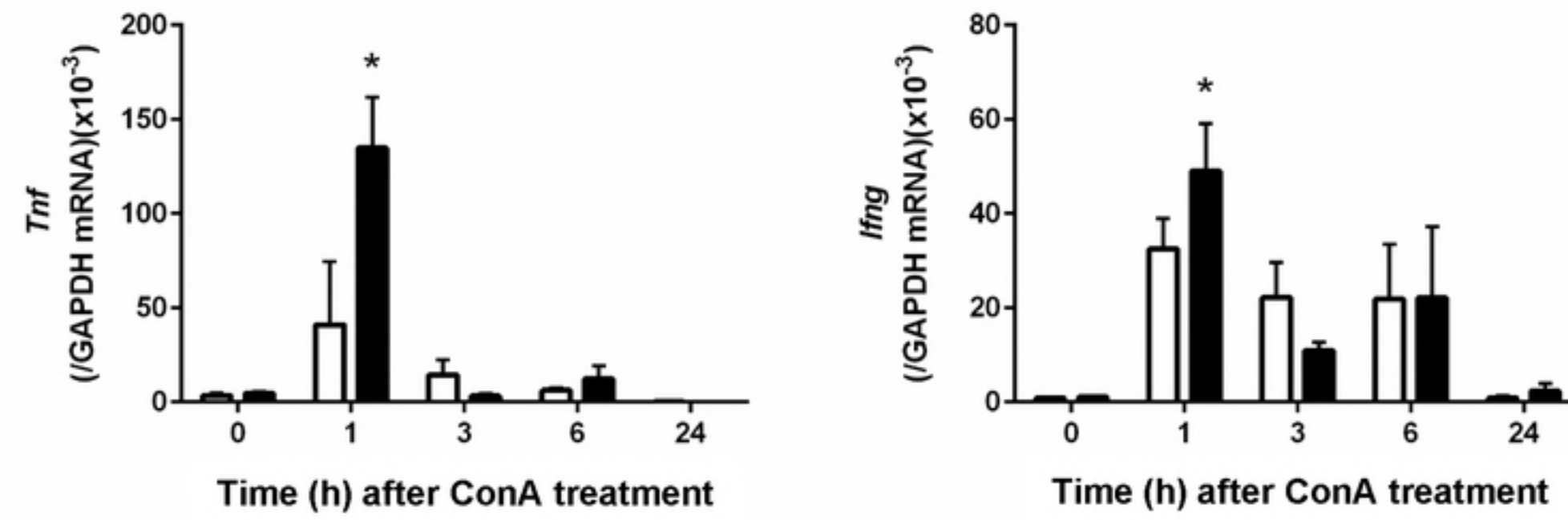

Fig 2

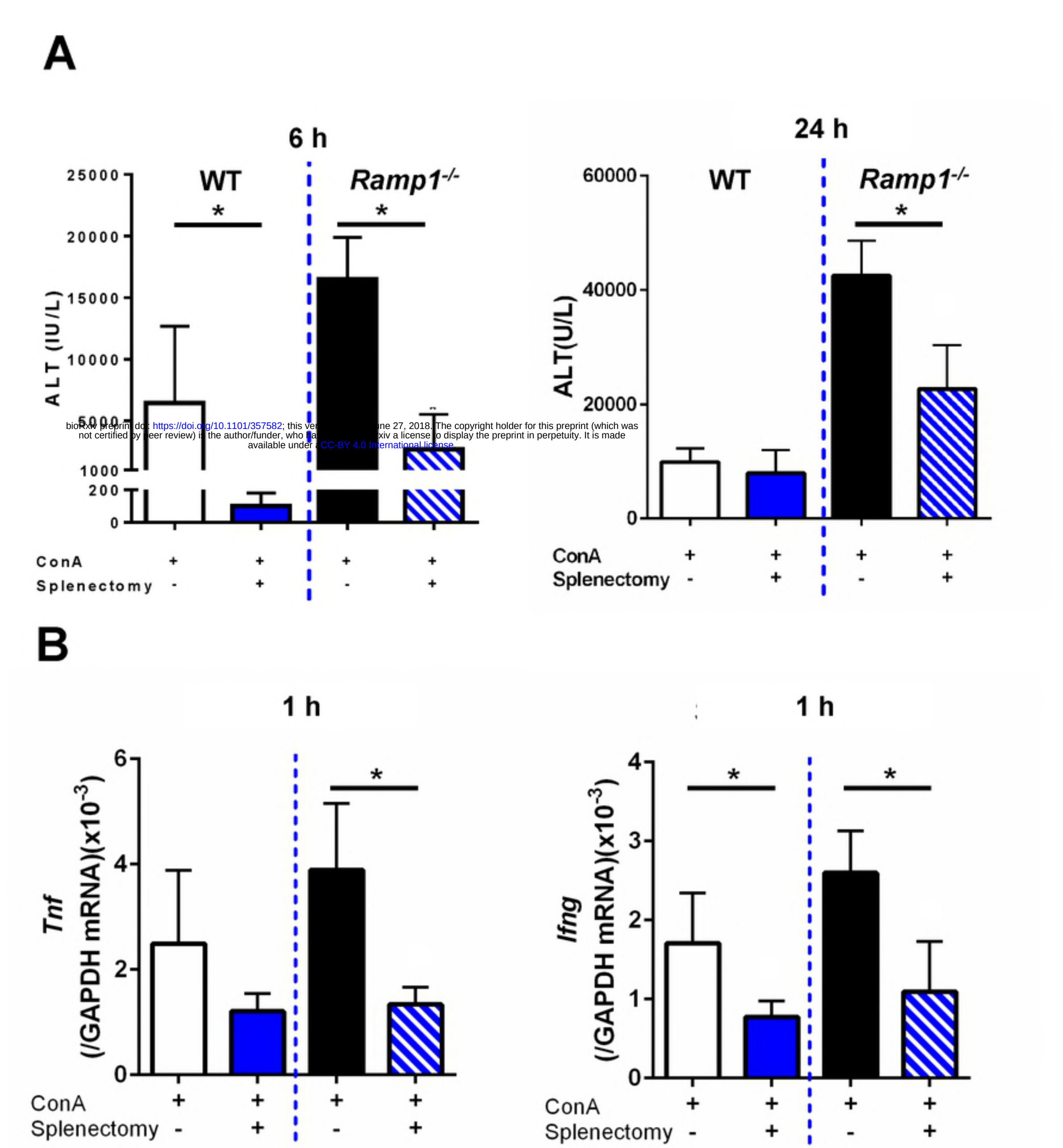

Fig 3

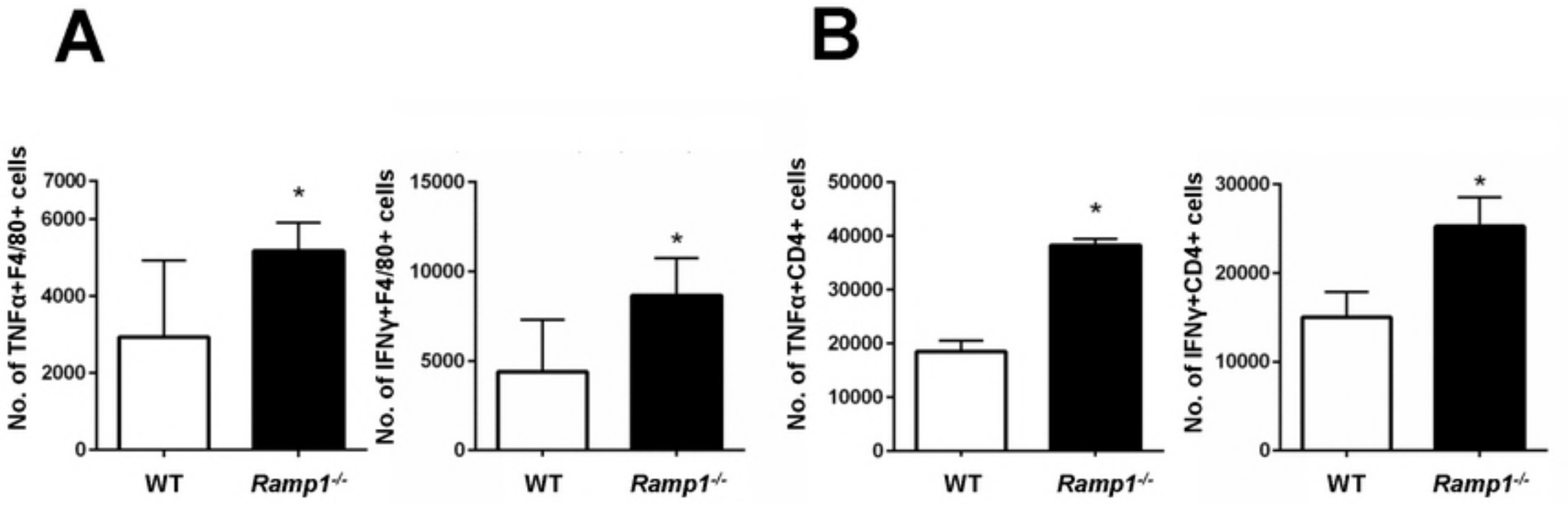

Fig 4

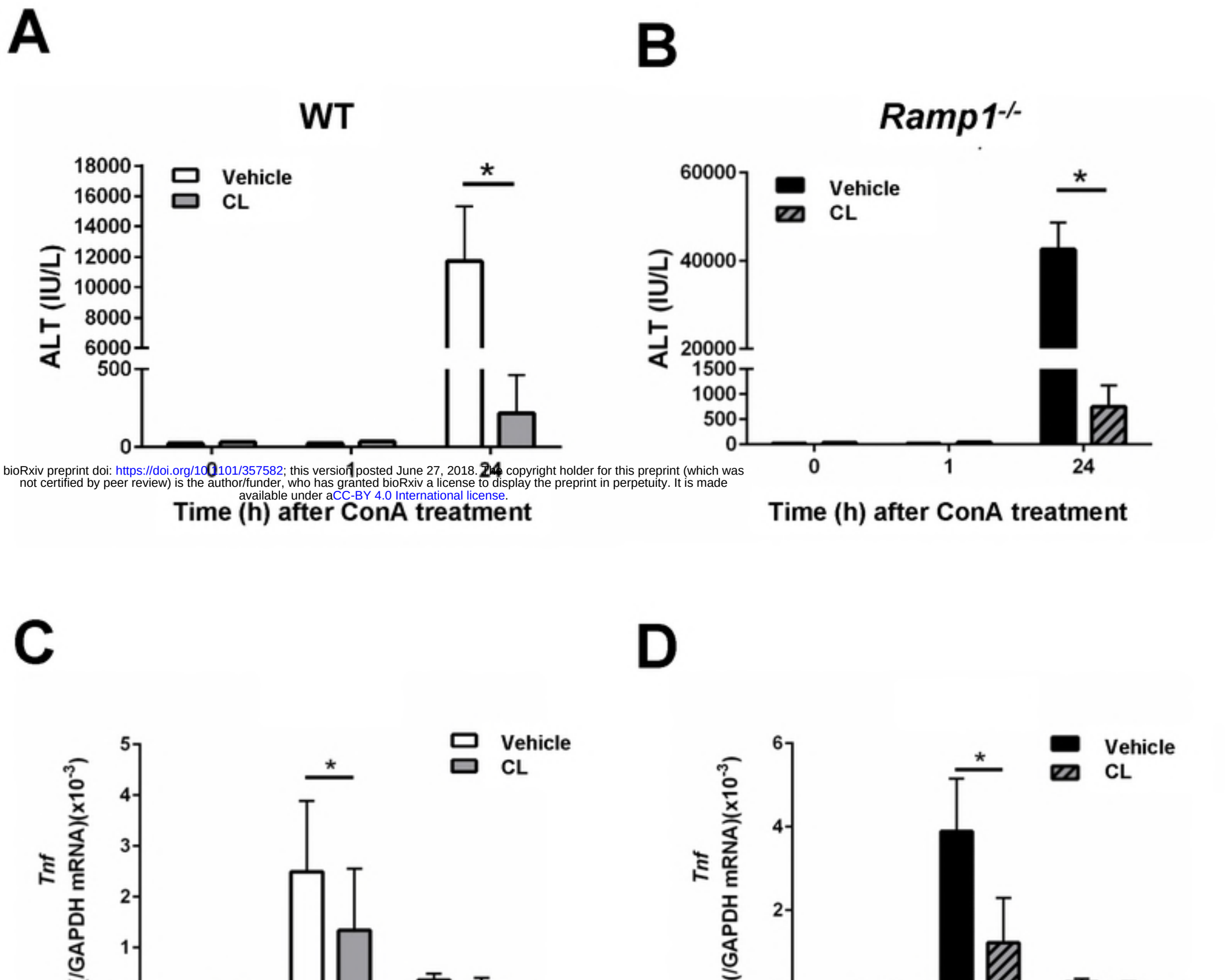

Fig 5

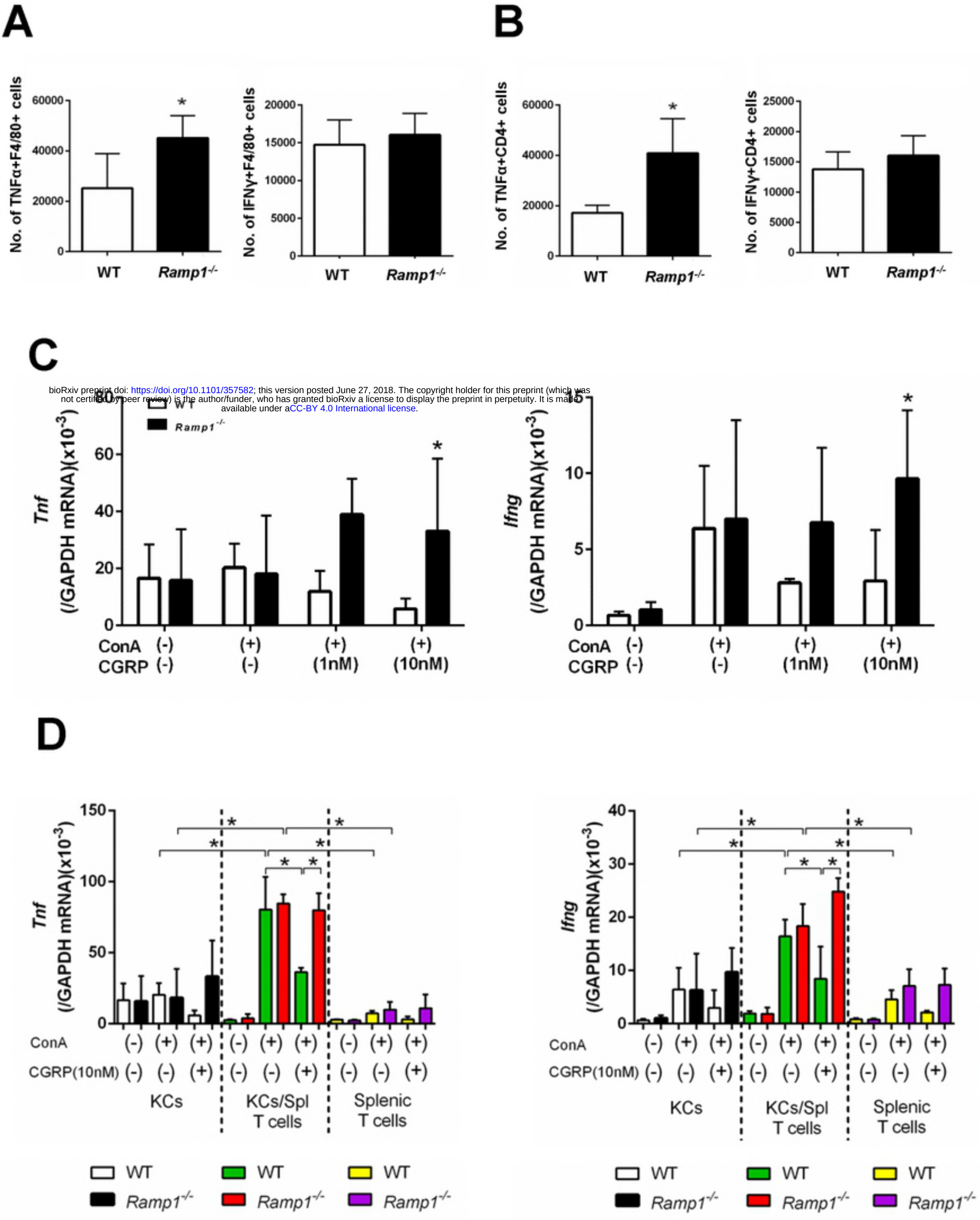

Fig 6

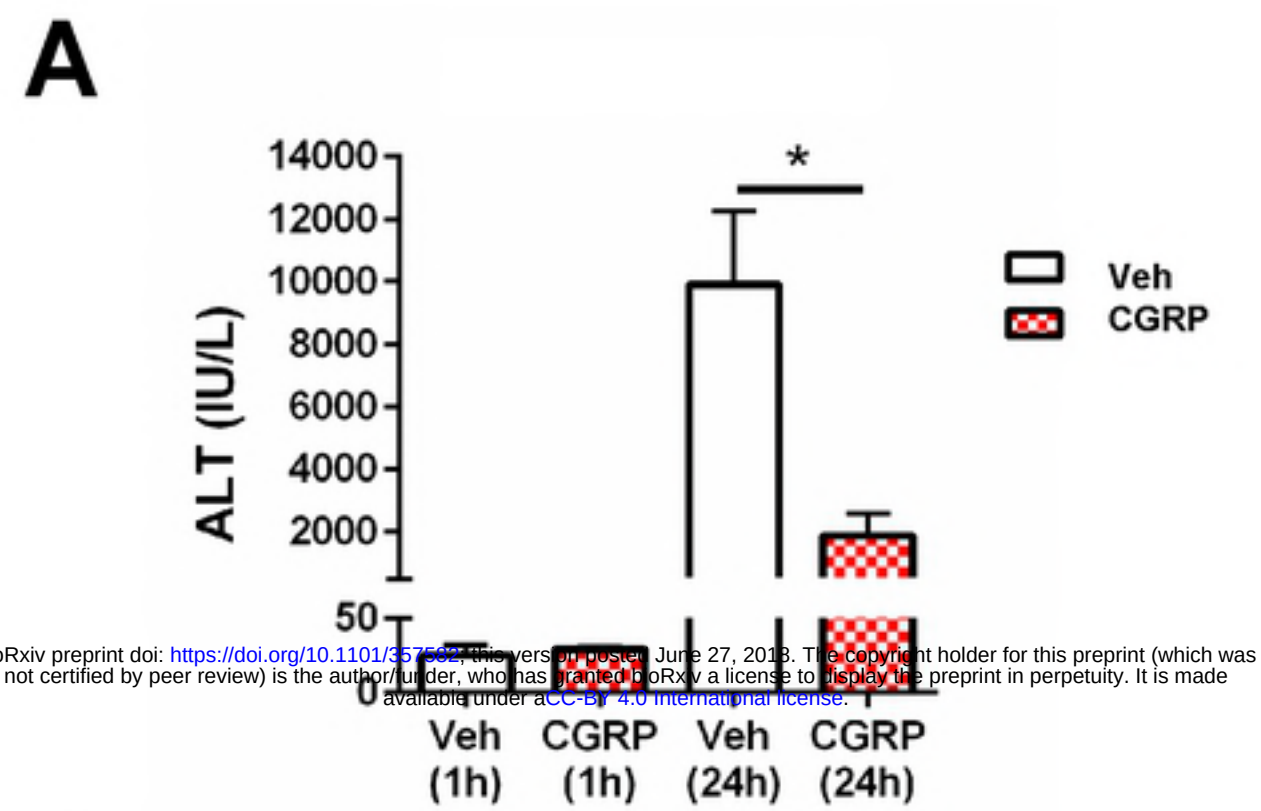

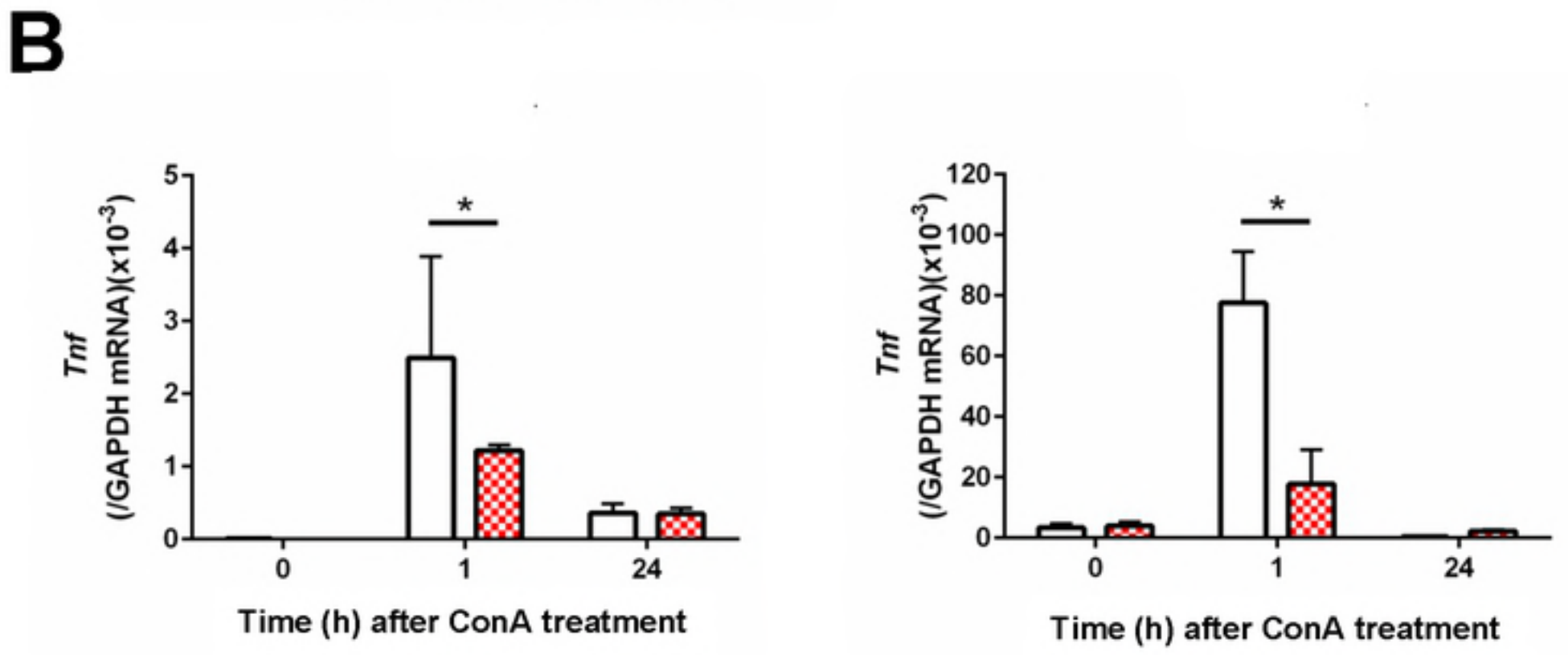

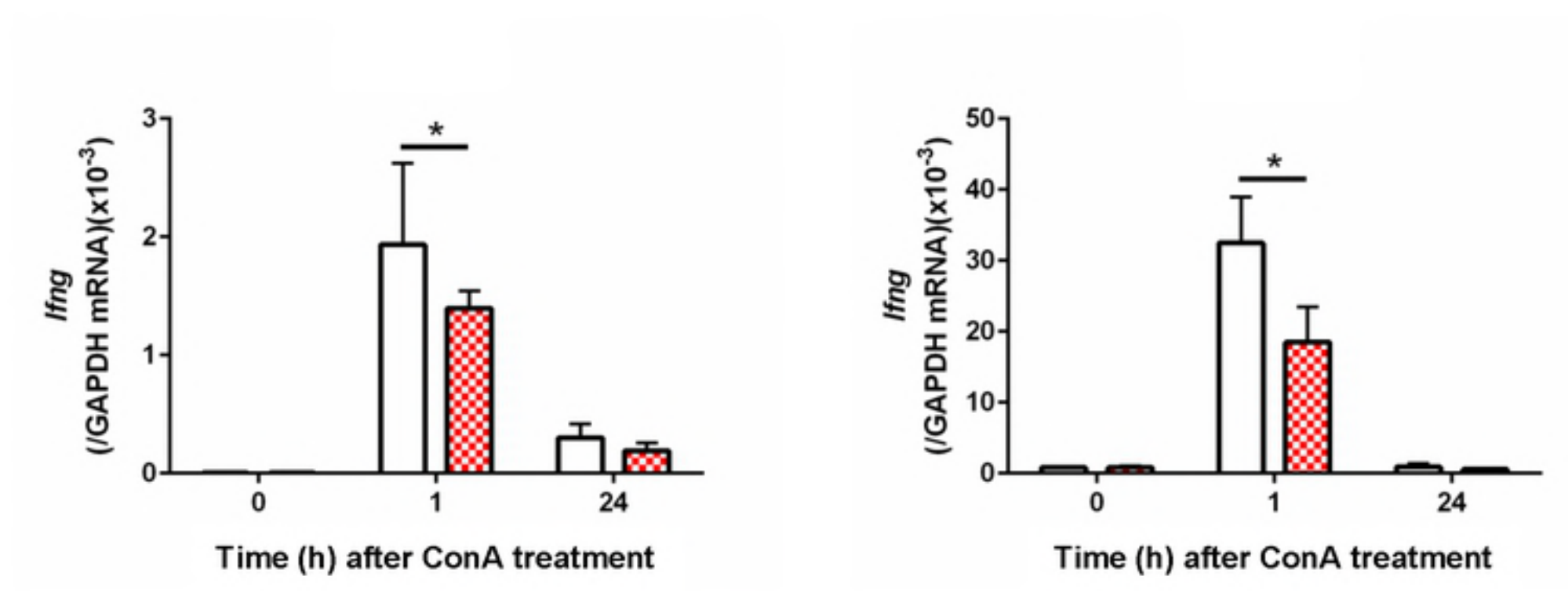

Fig 7